Chemical Engineering Research and Design 185 (2022) 281–290

Available online at www.sciencedirect.com

Chemical Engineering Research and Design

journal homepage: www.elsevier.com/locate/cherd

Comparison of analytical film theory and a numerical model for predicting concentration polarisation in membrane gas separation

K. Foo[a], Y.Y. Liang[a,*], P.S. Goh[b], A.L. Ahmad[c], D.K. Wang[d], D.F. Fletcher[d]

[a] College of Engineering, Universiti Malaysia Pahang, Lebuhraya Tun Razak, 26300 Gambang, Kuantan, Pahang, Malaysia

[b] Advanced Membrane Technology Research Centre (AMTEC), School of Chemical and Energy Engineering, Faculty of Engineering, Universiti Teknologi Malaysia (UTM), 81310 Skudai, Johor, Malaysia

[c] School of Chemical Engineering, Engineering Campus, Universiti Sains Malaysia, 14300 Nibong Tebal, Seberang Prai Selatan, Pulau Pinang, Malaysia

[d] The University of Sydney, School of Chemical and Biomolecular Engineering, NSW 2006, Australia

ARTICLE INFO

Article history:
Received 30 May 2022
Received in revised form 8 July 2022
Accepted 13 July 2022
Available online 15 July 2022

Keywords:
CFD
Membrane gas separation
Concentration polarisation
Analytical film theory
Gas permeation flux

ABSTRACT

Accurate prediction of the concentration polarisation (CP) effect is very important in the design of an efficient membrane-based gas separation process. This study analyses the reliability of analytical film theory (FT) for evaluating the performance of gas separation membranes in terms of CP and flux. The analytical model is compared against a more rigorous numerical model developed by using Computational Fluid Dynamics (CFD) for various operating variables. The results show that the FT prediction is less accurate at high CP conditions when gas permeation through the membrane increases, due to higher permeance selectivity and pressure ratio. Hence, the results suggest that FT is not recommended for membranes with high permeance or high-pressure conditions. Given that the typical range of feed composition and temperature has little impact on fluid properties (i.e., gas diffusion coefficient, densities, and viscosities), the resulting CP does not vary much and hence both FT and CFD models predict a similar CP. The analysis also suggests that the FT model is more accurate in predicting CP in the region closer to the membrane entrance. Overall, the analytical film theory serves as a reliable approximation in membrane gas applications under low CP at high crossflow and low flux conditions.

© 2022 Institution of Chemical Engineers. Published by Elsevier Ltd. All rights reserved.

1. Introduction

Concentration polarisation (CP) is one of the critical problems associated with membrane separation processes. CP occurs when the gradual accumulation of the rejected species takes place near the membrane surface due to the selective permeability of membranes (Al-Obaidi and Mujtaba, 2016; Matthiasson and Sivik, 1980). The increased CP would eventually reduce the driving force between the feed and permeate sides of the membrane, thus decreasing the membrane overall performance. In membrane gas separations, the phenomenon occurs when the concentration of the less permeable species increases in the boundary layer adjacent to the membrane surface as a result of rapid permeation of the more permeable species through the membrane (Baker, 2004). Early studies have confirmed that the polarisation effects cannot be neglected for gas separations, especially for membranes with high permeability (Bhattacharya and Hwang, 1997; Chen et al., 2011, 2012; He et al., 1999; Lüdtke et al., 1998; Mourgues and Sanchez, 2005; Takaba and Nakao, 2005; Zhang et al., 2006). Therefore, CP prediction is an important aspect in designing membrane-

* Corresponding author.
E-mail address: yongyeow.liang@ump.edu.my (Y.Y. Liang).

https://doi.org/10.1016/j.cherd.2022.07.014

0263-8762/© 2022 Institution of Chemical Engineers. Published by Elsevier Ltd. All rights reserved.

Nomenclature

Symbol

D	Diffusion coefficient ($m^2\ s^{-1}$).
d_h	Hydraulic diameter (m).
E_o	Enrichment term.
$f = \frac{d_h \Delta p_{ch}}{2\rho u_{avg}^2 L_m}$	Fanning friction factor.
h	Channel half-height (m).
h_{ch}	Membrane channel height (m).
j	Volumetric flux per unit area ($m^3\ m^{-2}\ s^{-1}$).
J	Mass flux ($kg\ m^{-2}\ s^{-1}$).
L_{in}	Entrance length (m).
L_m	Membrane length (m).
L_{out}	Exit length (m).
M	Molecular weight ($g\ mol^{-1}$).
n	Mole fraction.
p	Pressure (Pa).
P	Gas permeance ($mol\ m^{-2}\ s^{-1}\ Pa^{-1}$).
R	Ideal gas constant ($atm\ L\ mol^{-1}\ K^{-1}$).
$Re_h = \frac{\rho u_{avg} d_h}{\mu}$	Hydraulic Reynolds number.
Sc	Schmidt number.
t	Time (s).
T	Temperature (°C).
u_{avg}	Average velocity ($m\ s^{-1}$).
u_{b0}	Inlet velocity at any y-direction ($m\ s^{-1}$).
v_w	Fluid velocity normal to the wall ($m\ s^{-1}$).
$\vec{v}$	Velocity vector ($m\ s^{-1}$).
w	Mass fraction.
w_{ch}	Membrane channel width (m).
x	Distance in the bulk flow direction, parallel to membrane surface (m).
y	Distance from the bottom membrane surface, in direction normal to the surface (m).

Greek letters

α	Membrane selectivity.
δ	Film layer thickness (m).
γ	Concentration polarisation modulus.
μ	Dynamic viscosity ($kg\ m^{-1}\ s^{-1}$).
φ	Pressure ratio.
ρ	Density ($kg\ m^{-3}$).
τ	Wall shear stress (Pa).

Subscript

b	Value at inlet bulk conditions.
f	Value for the feed.
max	Value for maximum variable.
mix	Value for a binary gas mixture of CO_2 and CH_4.
o	Value on the feed side membrane surface (wall).
out	Value at the domain outlet.
p	Value for the permeate.

based gas separation processes and evaluating the performance of membranes.

Early theoretical models, such as the film theory (FT), were developed to describe CP phenomena by assuming the formation of a boundary layer of thickness (δ) associated with impermeable membrane walls (Baker, 2004; Michaels, 1968; Probstein et al., 1977; Zydney, 1997). In addition, the analytical model also simplifies the mass transport problem by assuming a uniform concentration along the membrane channel, such that the boundary layer thickness is independent of the transverse flow field (permeate flux). Nevertheless, no study up to now has discussed the accuracy of the film theory model against numerical simulations for describing CP in membrane-based gas separation.

Hence, this paper aims to analyse the reliability of analytical film theory and its limitations for evaluating the performance of gas separation membranes. The analytical model is compared against a more rigorous numerical model developed using computational fluid dynamics (CFD), which solves the flow and continuity equations for the gas separation system by taking into account the coupling of momentum and mass transport. The calculations are performed for typical CO_2/CH_4 gas separation (Feng et al., 2021; Liang et al., 2018, 2017), and the performance is analysed in terms of CP and flux by considering the effects of varying hydraulic Reynolds number (Re_h), membrane selectivity, feed composition, temperature, as well as pressure ratio in the membrane system.

2. Methodology

2.1. *Theoretical background of CP analytical model by film theory*

Current commercial membrane gas separation processes mainly use dense polymeric membranes. The separation of gas mixtures through the dense membrane film is generally described by the solution-diffusion mechanism, where a gas component dissolves into the membrane material and then permeates through the dense film down a concentration gradient (Baker, 2004). The transport of gas components within the boundary layer at any point in the membrane feed channel can be expressed by using Fick's law as follows:

$$\rho j_f w_i - \rho D \frac{\partial w_i}{\partial y} = \rho j_p w_{i,p} \tag{1}$$

where ρ is the density, w_i is the mass fraction of gas species i, D is the diffusion coefficient, j_f and j_p are the volume fluxes of gas ($m^3\ m^{-2}\ s^{-1}$) on the feed and permeate sides of the membrane, respectively.

In gases, the volume fluxes on the feed and permeate sides of the membrane are not the same. Nevertheless, the gas volume fluxes can relate with each other by correcting for the feed and permeate pressures, p_f and p_p on each membrane side as follows:

$$j_f p_f = j_p p_p \tag{2}$$

This gives

$$j_f \frac{p_f}{p_p} = j_f \varphi = j_p \tag{3}$$

where φ is the pressure ratio (p_f/p_p) of the membrane system. Using the definition of pressure ratio to relate the gas volume fluxes on each membrane side in Eq. (1) gives the following expression

$$-\rho D \frac{\partial w_i}{\partial y} = \rho j_f (\varphi w_{i,p} - w_i) \tag{4}$$

The mass balance Eq. (4) can be integrated over the boundary layer thickness (δ) to give a concentration polarisation equation (Brian, 1965) as follows:

Table 1 – Mathematical formulation used for estimation of gas mixture properties.

Gas properties	Theory of formula	Mathematical equation
Diffusion coefficient, D ($m^2\ s^{-1}$)	Chapman and Enskog theory (Cussler, 1997).	$D = \frac{1.86\times10^{-3}T^{3/2}\left(1/M_i + 1/M_j\right)^{1/2}}{p\sigma_{ij}^2\Omega}$
Density of gas mixture, ρ_{mix} ($kg\ m^{-3}$)	Ideal gas law (Moran and Shapiro, 1988).	$\rho_{mix} = \frac{1}{\Sigma\left(\frac{w_i}{\rho_i}\right)_n}$
Dynamic viscosity of gas mixture, μ_{mix} ($kg\ m^{-1}\ s^{-1}$)	Wilke correlation (Wilke, 1950).	$\mu_{mix} = \frac{\Sigma\left(\mu_i n_i \sqrt{M_i}\right)}{\Sigma\left(n_i\sqrt{M_i}\right)}$

$$\frac{w_{i,o}/\varphi - w_{i,p}}{w_{i,b}/\varphi - w_{i,p}} = \exp\left(\frac{j_f\delta}{D}\right) \tag{5}$$

Alternatively, the concentration terms in Eq. (5) can be replaced using the membrane enrichment terms, E and E_o. The enrichment terms represent the factors which determine the magnitude of concentration polarisation based on the difference in gas permeabilities (Baker, 2004). As the difference in gas permeabilities increases, the membrane enrichment terms increase, resulting in larger concentration gradients and thus higher CP. The enrichment terms for gases are generally expressed as volume fractions in terms of the pressure ratio (φ), such that

$$E = \frac{w_{i,p}}{w_{i,b}}\cdot\varphi \tag{6}$$

Excluding the presence of a boundary layer, E_o is expressed as

$$E_o = \frac{w_{i,p}}{w_{i,o}}\cdot\varphi \tag{7}$$

It must be noted that both enrichment terms for CO_2 are larger than one because the membrane selectively permeates the gas component. Substituting the enrichment terms into Eq. (5) gives

$$\frac{1 - 1/E_o}{1 - 1/E} = \exp\left(\frac{j_f\delta}{D}\right) \tag{8}$$

The extent of concentration polarisation is measured by the magnitude of the ratio between the permeate concentration at the membrane surface ($w_{i,o}$) compared with the bulk concentration ($w_{i,b}$). Hence, CP effect becomes significantly important when the CP modulus ($\gamma = w_{i,o}/w_{i,b}$) deviates from one. In this case, the CP modulus is represented by the concentration gradient of the more permeable CO_2 gas component. By using the definitions of E and E_o, the CP modulus can be expressed as

$$\gamma = \frac{E}{E_o} = \frac{w_{i,o}}{w_{i,b}} = \frac{\exp(j_f\delta/D)}{1 + E_o[\exp(j_f\delta/D) - 1]} \tag{9}$$

Later the gas volume flux is predicted by CFD calculations and used as an input in CP prediction for the analytical solution as in Eq. (9). For a fully developed laminar flow in a narrow rectangular channel with soluble walls (Probstein, 1989), the boundary layer thickness can be expressed as

$$\frac{\delta(x)}{x} = 1.475\left(\frac{h}{x}\right)^{2/3}\left(\frac{D}{u_{max}h}\right)^{1/3} \tag{10}$$

where x is the longitudinal coordinate, h is the channel half-height, and u_{max} is the maximum crossflow velocity at the centre of channel. The equations and theories used for estimating gas mixture properties are listed in Table 1:

2.2. *Flux calculations for membrane gas separation*

In gas separation, the driving force across the membrane is driven by the partial pressure difference of the gas component across the membrane, which can be expressed as follows:

$$J_i = P_i(p_{i,o} - p_{i,p}) \tag{11}$$

where J_i is the mass flux of gas species i ($kg\ m^{-2}\ s^{-1}$), P_i is the gas permeance, $p_{i,o}$ and $p_{i,p}$ are the partial pressures of the gas species on the feed and permeate sides of the membrane, respectively. Note that the total gas pressures on a membrane side (either feed or permeate) are the summation of gas partial pressures for a mixture of species i and j, respectively. The partial pressures are related to the mole fractions of the gas species on both sides of the membrane and can be calculated as

$$n_{i,o} = \frac{p_{i,o}}{p_o}, \quad n_{i,p} = \frac{p_{i,p}}{p_p} \tag{12}$$

Hence, the flux Eq. (11) can be rewritten as

$$J_i = P_i(n_{i,o}p_o - n_{i,p}p_p) \tag{13}$$

and $n_{i,p}$ is determined using the following expression by relating the concentration of gas species i on both sides of the membrane (i.e. feed and permeate sides) (Baker, 2004):

$$n_{i,p} = \frac{\varphi}{2}\left[n_{i,o} + \frac{1}{\varphi} + \frac{1}{\alpha - 1} - \sqrt{\left(n_{i,o} + \frac{1}{\varphi} + \frac{1}{\alpha - 1}\right)^2 - \frac{4\alpha n_{i,o}}{(\alpha - 1)\varphi}}\right] \tag{14}$$

where α is the membrane selectivity. Membrane selectivity (α) is a quantification of the ability of a membrane to separate two gases, i and j, and can be expressed as

$$\alpha = \frac{P_i}{P_j} \tag{15}$$

Table 2 summaries the differences between the numerical solution using the CFD approach and the film theory (FT) approximation as follows:

Table 2 – Summary of the differences between the numerical approach and the film theory approximation.

Description	Numerical solution (CFD simulation)	FT approximation	Significance and source of difference
Concentration polarisation (CP) and permeate flux	Can be calculated directly by solving the mass transport of gas component within the local boundary layer using Fick's law.	Requires gas concentration and flux input data from either experimental or numerical simulation for calculations of CP and permeate flux.	The effect of varying solute permeation on CP for FT approximation is not considered.
Flow profiles	Resolves the local velocity distribution within the fluid domain.	The local velocity profiles cannot be predicted directly.	CFD requires higher computational effort.

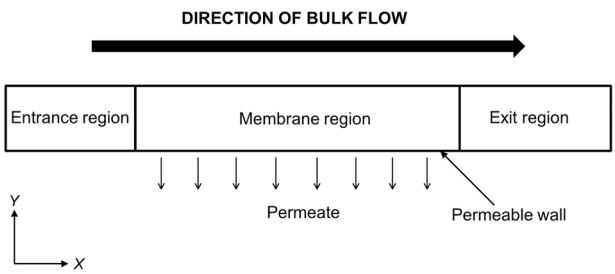

Fig. 1 – Schematic diagram of CFD fluid domain (not to scale) for modelling of a gas separation feed channel.

2.3. *Description of numerical model by CFD*

Fig. 1 shows a schematic diagram of the 2D CFD fluid domain used for modelling CO_2/CH_4 gas separation in this paper. An empty rectangular channel is constructed for the fluid domain (Fig. 1), which is a simplified geometry of a hollow fibre membrane channel (Liang et al., 2018). A membrane length (L_m) of 1 m is used for the fluid domain as it is the typical dimension used in commercial hollow fibre gas separation modules (Ahmad et al., 2015). The length of the entrance region is set as one-fifth of the membrane length (1/5 × L_m), and it is doubled for the exit region (2× entrance length). These regions are located at each end of the membrane channel to avoid the flow solution being affected by both inlet and outlet boundary conditions (see Fig. 1) (Schwinge et al., 2002a,b).

2.3.1. *Boundary conditions*

The present study employs the commercial CFD code, ANSYS CFX-18.2 for simulating an isothermal two-dimensional (2D) flow with constant Newtonian fluid properties inside an empty rectangular channel (Fletcher and Wiley, 2004). The steady-state simulations are performed with negligible gravitational effects and the binary gas mixture (i.e. CO_2 and CH_4 gas) treated as an incompressible fluid (Fletcher and Wiley, 2004; Wiley and Fletcher, 2003). The governing Navier-Stokes equations are therefore, given as in Eqs. (16)–(18), while the mass transport equation for gas species i is expressed in the form of Eq. (19) as follows:

$$\frac{\partial u}{\partial x} = -\frac{\partial v}{\partial y} \tag{16}$$

$$\rho\frac{\partial u}{\partial t} + \rho\left(u\frac{\partial u}{\partial x} + v\frac{\partial u}{\partial y}\right) = \mu\left(\frac{\partial^2 u}{\partial x^2} + \frac{\partial^2 u}{\partial y^2}\right) - \frac{\partial p}{\partial x} \tag{17}$$

$$\rho\frac{\partial v}{\partial t} + \rho\left(u\frac{\partial v}{\partial x} + v\frac{\partial v}{\partial y}\right) = \mu\left(\frac{\partial^2 v}{\partial x^2} + \frac{\partial^2 v}{\partial y^2}\right) - \frac{\partial p}{\partial y} \tag{18}$$

$$\frac{\partial w_i}{\partial t} + u\frac{\partial w_i}{\partial x} + v\frac{\partial w_i}{\partial y} = D\left(\frac{\partial^2 w_i}{\partial x^2} + \frac{\partial^2 w_i}{\partial y^2}\right) \tag{19}$$

The high-resolution schemes were chosen for solving the partial differential Eqs. (16)–(19) to reduce numerical diffusion. All steady-state simulations are considered to have converged once the RMS errors for residuals drop below 10^{-10}.

The local mass fraction of gas species i and pressure at any point of the membrane wall can be obtained directly from CFD calculations. A parabolic velocity profile is specified at the feed inlet, whereas the outlet boundary is set to zero relative pressure. The top surface and other non-membrane channel walls, i.e., entrance and exit region walls, are treated as no-slip walls with zero mass flux condition. Table 3 summarises the mathematical expressions used for the boundary conditions specified at different locations of fluid domain boundaries.

2.3.2. *Assumption and cases*

Mesh independence studies are performed for model verification so that any potential source of numerical errors due to inadequate mesh resolution can be excluded. Typically, a grid resolution with a convergence index (GCI) value below 5 % is sufficient for verification studies (Fimbres-Weihs and Wiley, 2010; Roache and Knupp, 1993). This was obtained when the fluid domain was discretised with a structured mesh using a minimum element size of 0.2 % and a maximum of 1.6 % of the membrane channel height, respectively. In addition, a minimum of 10 inflation layers are applied near the membrane surfaces (with the first layer thickness being approximately 0.1 % of the membrane channel height) to properly resolve the velocity and concentration boundary layers. Overall, a fluid domain comprising 1.6 million control volumes is used for which the resulting GCI was below 1 % for both permeate flux and friction factor.

Once the steady-state simulation has converged, the local variables, i.e., gas permeation flux and CP modulus, are calculated as the area-averaged variables within the membrane region length (L_m) using the following expression:

$$\bar{\phi} = \frac{1}{L_m}\int \phi dL_m \tag{20}$$

Tables 4 and 5 describe the reference parameters and operating variables used for the typical CO_2/CH_4 gas separation case studies. It is important to note that all operating variables (as in Table 5) are investigated considering other parameters to be the same following the reference case as indicated in Table 4. The permeate pressure (p_p) is set as constant at atmospheric pressure (see Table 4), which is commonly applied in membrane gas separation system (Saedi et al., 2014; White et al., 1995). It should be noted that

Table 3 – Mathematical expressions for boundary conditions of CFD model at different locations.

Boundary location	Boundary condition	Mathematical expression
Inlet	Specified parabolic velocity profile (u_{b0}) and concentration profile (w_{b0}).	$u_{b0} = 6u_{avg}(y/h_{ch})[1-(y/h_{ch})]$ $w_{b0} = w_{i,b}$
Outlet	Specified zero average reference pressure coupled with no-slip and zero mass flux condition.	$\frac{\partial w}{\partial x} = 0,\ p = p_{out}$
Membrane bottom wall	Specified fluid velocity normal to the wall (v_w) based on Fick's law of diffusion (Baker, 2004).	$v_w = \frac{J_p}{\rho}$
Symmetry plane	Specified zero velocity and concentration gradients in direction normal to plane.	$\frac{\partial \vec{v}}{\partial z} = 0,\ \frac{\partial w}{\partial z} = 0$
Membrane top surface and non-membrane channel walls	Set as no-slip walls with zero mass flux.	$\vec{v} = 0,\ \frac{\partial w}{\partial y} = 0$

Table 4 – Reference parameters used for gas separation case studies.

Reference parameters	Value
Permeate pressure, p_p (Pa)	101325
Pressure ratio, $\varphi = p_f / p_p$	15
Membrane selectivity, $\alpha = P_i / P_j$	25
Gas permeance of CH_4, P_j (mol m^{-2} s^{-1} Pa^{-1})	1×10^{-10}
Hydraulic diameter, d_h (m)	0.01
Hydraulic Reynolds number, $Re_h = \rho\ u_{avg}\ d_h / \mu$	200
Schmidt number, $Sc = \mu / \rho\ D$	0.66
Feed concentration of CO_2, $n_{i,b0}$	0.5
Temperature, T (°C)	25

Table 5 – Operating variables used for CO_2/CH_4 gas separation case studies.

Operating variables	Value
Membrane selectivity, $\alpha = P_i / P_j$	10 – 250
Pressure ratio, $\varphi = p_f / p_p$	5 – 65
Hydraulic Reynolds number, $Re_h = \rho\ u_{avg}\ d_h / \mu$	100 – 800
Feed concentration of CO_2, $n_{i,b0}$	0.05 – 0.9
Temperature, T (°C)	25 – 60

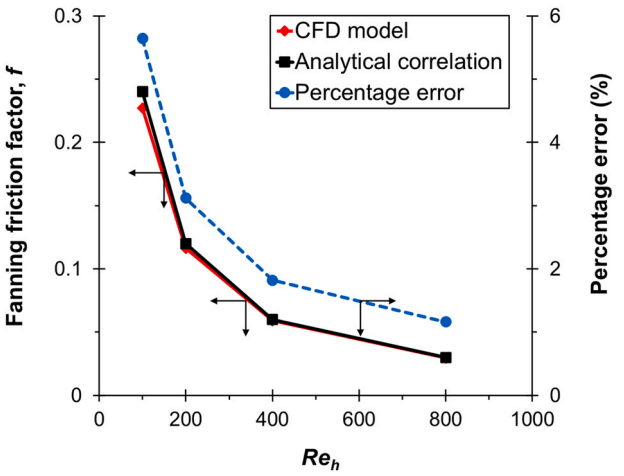

Fig. 2 – Effect of hydraulic Reynolds number on Fanning friction factor and prediction error (%) between CFD model and analytical correlation.

feed pressure (p_f) is varied based on the value of pressure ratio as in Table 5. The permeance value of CH_4 (P_j) is fixed for all case studies considered (as in Table 4), while the permeance value of CO_2 (P_i) is varied depending on membrane selectivity (α), as indicated in Table 5 (Blinova and Svec, 2012; Cakal et al., 2012; Yu et al., 2022).

2.3.3. *Comparison between CFD model and analytical correlation*

In order to ensure model accuracy, the CFD model presented in this study is compared against the hydrodynamics analytical correlation, i.e. Fanning friction factor (f) at different Reynolds number. The Fanning friction factor calculated by CFD in an empty membrane channel is given as follows (Bird et al., 1960):

$$f = \frac{d_h \Delta p_{ch}}{2\rho u_{avg}^2 L_m} \tag{21}$$

where d_h is the hydraulic diameter, Δp_{ch} is the channel pressure drop, u_{avg} is the average velocity, and L_m is the membrane length.

For a fully developed laminar flow in 2D rectangular channels without permeation through membrane, the analytical correlation for calculating friction factor is expressed as (Bird et al., 1960):

$$f = \frac{24}{Re} \tag{22}$$

Fig. 2 shows that both CFD and analytically calculated friction factors agree well with each other with a maximum percentage difference of 5.6 % as Re increases. The friction factor predicted by CFD is consistently smaller compared with that of the analytical correlation (Fig. 2). This is because the gas permeation across the membrane in the CFD model causes a reduction of bulk fluid flow in the membrane channel, leading to a decrease in the u-velocity gradient normal to the membrane wall, and hence lower friction factor (Liang et al., 2014, 2016). Fig. 2 also shows that the percentage difference in f prediction is larger at smaller Re. This is expected, as the membrane extracts more fluid relative to the bulk flow at a smaller Re. As the main driver of flux enhancement is driven by hydrodynamics, this gives confidence in the CFD model prediction.

3. Results and discussion

3.1. *Comparison of CP modulus and flux predicted by FT and CFD models*

Fig. 3 shows that the analytical film theory (FT) model results in a larger area-averaged CP modulus ($\bar{\gamma}$) compared with that predicted using the CFD model, thus indicating that the FT model consistently underestimates CP in the membrane system. As gas permeation increases across the membrane

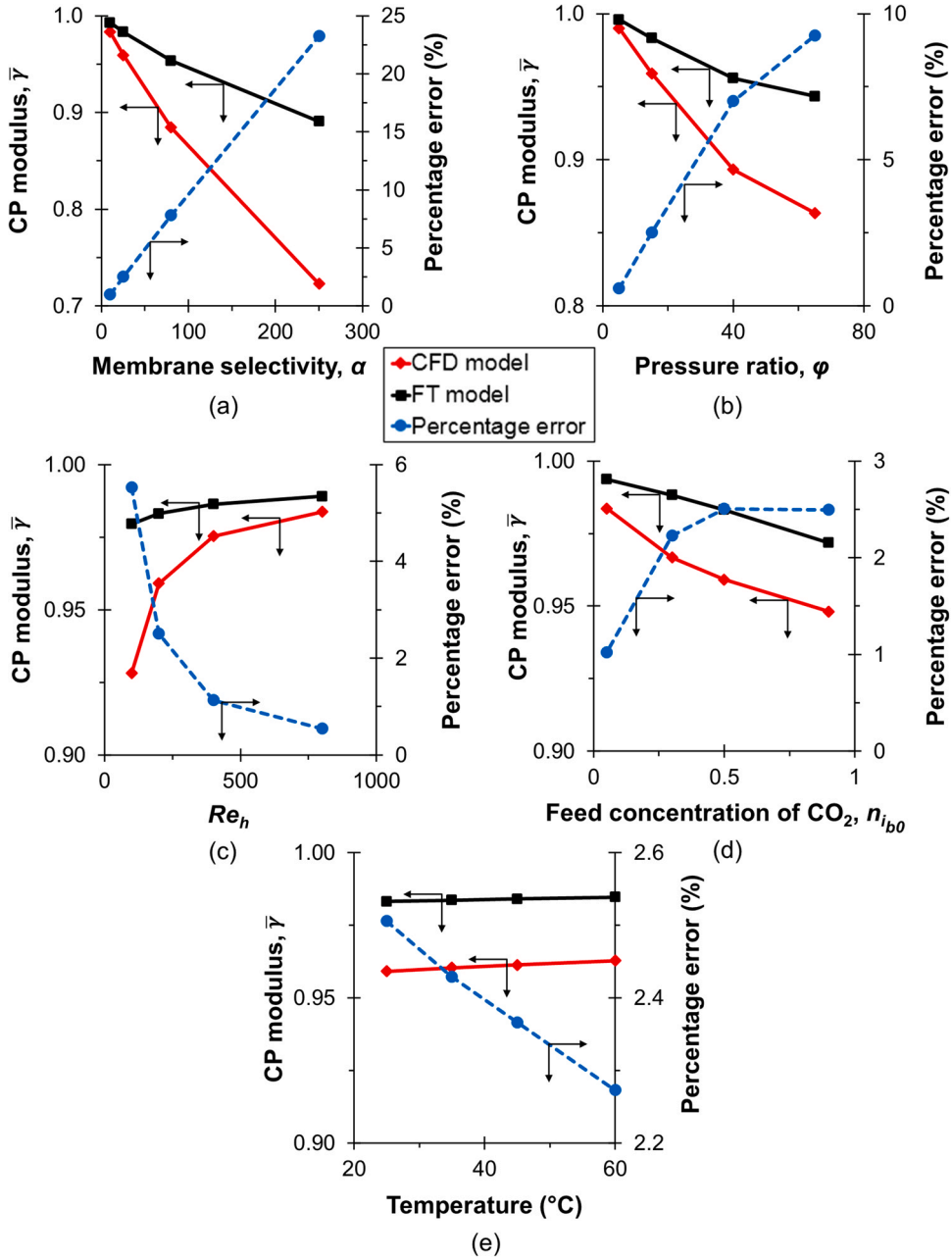

Fig. 3 – Effects of (a) membrane selectivity, (b) pressure ratio, (c) hydraulic Reynolds number, (d) feed composition, and (e) temperature on area-averaged modulus of concentration polarisation and prediction error (%) between analytical film theory (FT) and numerical (CFD) models.

due to higher membrane selectivity (gas permeance) and pressure ratio, this causes a large difference in CP predictions up to 25 % between the FT and CFD models (Fig. 3a and b).

Given that the FT model continues to underpredict CP, this leads to overestimation of gas permeate flux ($\bar{J}_{CO_2}$) in the membrane system, causing the flux predictions to deviate significantly as selectivity increases, i.e., up to 33 % difference between the models (Figure 4a). The significant deviation in predicting CP and flux by the FT model is related to its assumption that the boundary layer thickness does not depend on gas permeation, which undermines the effect of CP on the overall mass transfer performance in the membrane system. Hence, these results suggest that the FT model is not recommended for membranes with high permeance or high-pressure conditions. Note that the pressure ratio implemented in industrial gas applications is not more than 15, due to high cost of the energy requirement when compared with a slightly increased membrane gas separation rate (Huang et al., 2014). This implies that the present FT model can serve as a reliable prediction as the results agree well with that of CFD for the pressure ratio recommended in practical gas applications, in terms of CP and flux (Figs. 3b and 4b).

While the FT prediction is less accurate at high CP conditions typically, the difference in CP and flux predictions between the models, on the other hand, becomes smaller as the flow velocity (or Reynolds number, Re_h) increases, i.e. less than 1 % for CP, and 2 % for gas permeate flux, as shown in Figs. 3c and 4c, respectively. Given that the typical range of feed composition and temperature has little impact on fluid properties, i.e., gas diffusion coefficient, densities, and viscosities (Perry and Green, 2007), the resulting CP and flux do not vary much as well. Therefore, both models predict the membrane performance similarly with the difference in CP

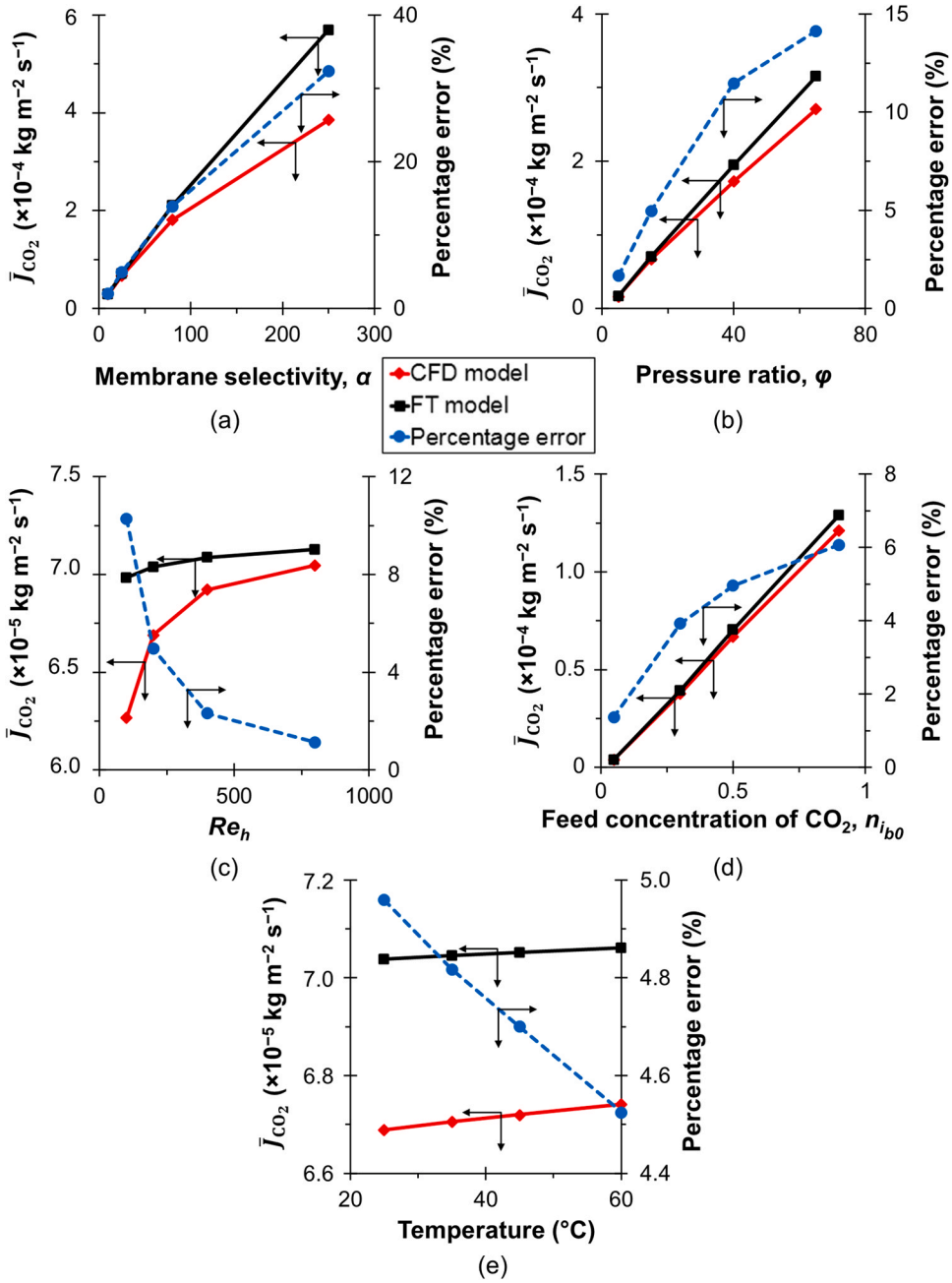

Fig. 4 – Effects of (a) membrane selectivity, (b) pressure ratio, (c) hydraulic Reynolds number, (d) feed composition, and (e) temperature on area-averaged permeate flux of CO_2 gas and prediction error (%) between analytical film theory (FT) and numerical (CFD) models.

and flux predictions is not more than 3 % (Fig. 3d and e) and 6 % (Fig. 4d and e), respectively.

3.2. *Accuracy of analytical film theory in industrial membrane gas separation*

In order to assess the accuracy of analytical film theory in industrial membrane gas separation, this section further compares the FT and CFD models across a series of operating variables, such as hydraulic Reynolds number, membrane selectivity, and pressure ratio that are typically encountered in industrial membrane processes. Table 6 lists the simulation parameters used for comparison between the models. A range of hydraulic Reynolds number (Re_h) from 100 to 800 is considered, which are typically applied in industrial gas separation membrane processes (Alkhamis et al., 2015; He, 2018). Given that the typical range of feed composition and temperature has little effect on CP and flux as mentioned in Section 3.1, a constant temperature of 25 °C and 0.5 mole fraction of feed gas concentration are used in this case.

Table 6 – Simulation parameters used for comparison between FT and CFD models.

Case	1	2	3	4	5	6	7	8	9	10
Re_h	100	200	400	800	200	200	200	200	200	200
α	25	25	25	25	10	80	250	25	25	25
φ	15	15	15	15	15	15	15	5	40	65

Fig. 5 shows the predictions of CP modulus and gas permeate flux by the FT model plotted against CFD results. It

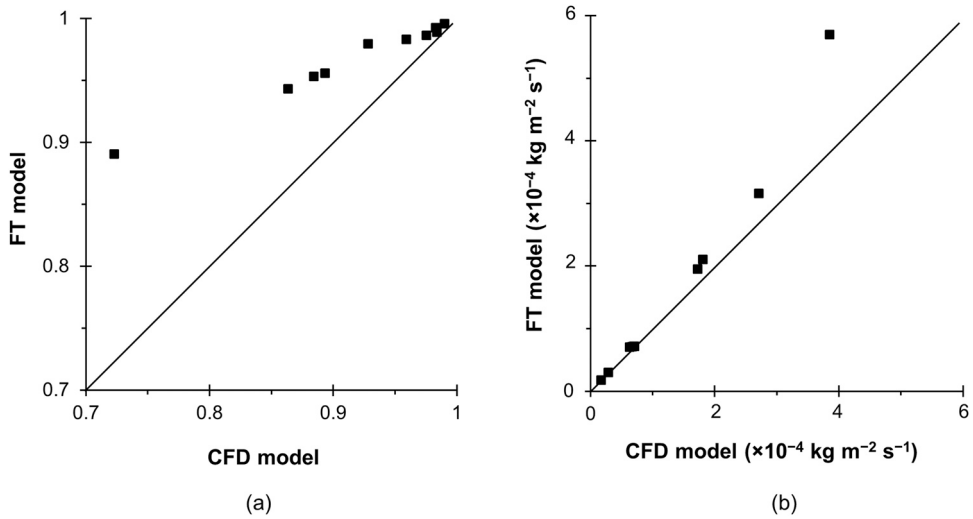

Fig. 5 – Comparison of predictions between analytical film theory (FT) and numerical (CFD) models for area-averaged (a) CP modulus and (b) CO_2 permeate flux. The temperature and feed concentration of CO_2 (mole fraction) are constant at 25 °C and 0.5, respectively for simulation conditions stated in Table 6.

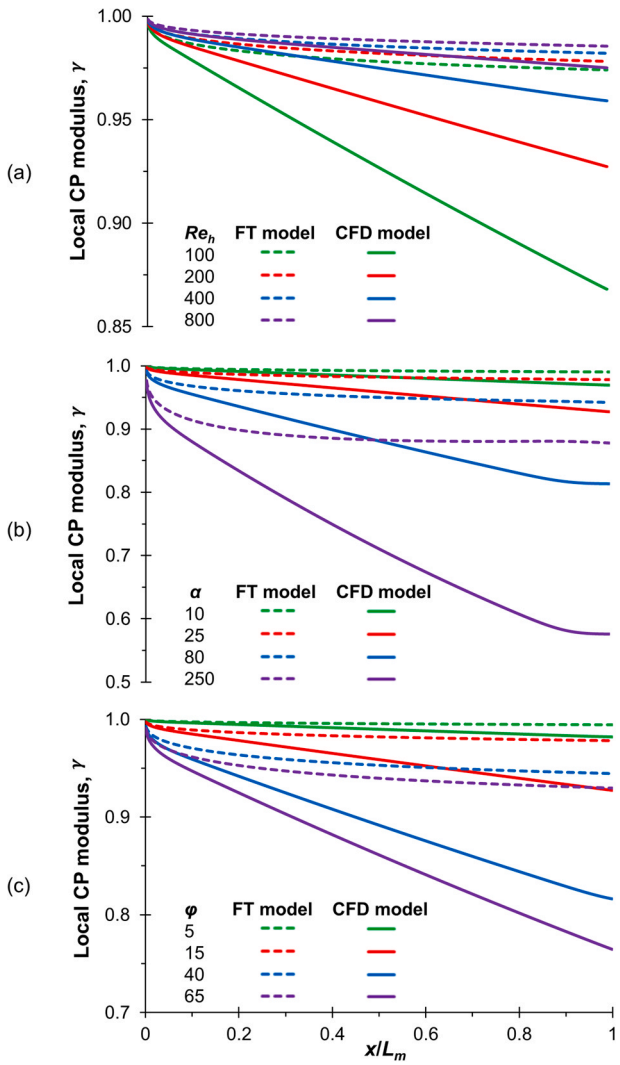

Fig. 6 – Effects of (a) hydraulic Reynolds number, (b) membrane selectivity, and (c) pressure ratio on local CP modulus estimated by analytical film theory (FT) and numerical (CFD) models along the membrane channel.

is found that there is an average difference of 5.2 % in CP modulus predicted by both models as the FT model consistently underestimates CP, i.e., below 0.9 of CP modulus as shown in Fig. 5a. This in turn causes the FT model to overestimate the CO_2 permeate flux and the difference becomes larger at fluxes higher than 2×10^{-4} kg m^{-2} s^{-1}, resulting in an average difference of 9.4 % and a maximum deviation of 32.4 % in flux predictions between the models (Fig. 5b).

3.3. *Estimation of local concentration polarisation by film theory*

Accurate prediction of local CP becomes important in membrane gas separation process as significant CP phenomena would reduce gas permeation flux, thus decreasing the overall performance of membrane module. The local CP modulus (γ) can be estimated by using the analytical FT model and is expressed as

$$\gamma(x) = \frac{\exp\left(j_f(x)\cdot\delta(x)/D_i\right)}{1 + E_o\left[\exp\left(j_f(x)\cdot\delta(x)/D_i\right) - 1\right]} \tag{23}$$

where $j_f(x)$ is the local feed volumetric flux calculated by CFD model, and $\delta(x)$ is the local boundary layer thickness which can be obtained from Eq. (10).

Fig. 6a shows that the difference in local γ predictions between the FT and CFD models decreases along the membrane channel at higher Re_h. This is because a higher Re_h enhances flow mixing and results in an increase in the boundary layer renewal near the membrane surface, which minimises CP in the membrane system, leading to a smaller difference in the local γ predictions between both models. Hence, a further increase in Re_h is expected to result in a closer prediction between the FT and CFD models in this case. Fig. 6b and c, on the other hand, show that the difference in local γ predictions increases as membrane selectivity and/or pressure ratio increases. Overall, the trends obtained

in Fig. 6 show that the difference in local γ predicted between both models becomes larger along the membrane channel. This suggests that the CP prediction using the FT model is more reliable in the region closer to the entrance of membrane channel.

It should be noted that although this study is performed for typical CO_2/CH_4 gas separation, the insights drawn from this work are applicable to all gases as the mass transfer finding is driven by hydrodynamics, rather than the gas species. Nevertheless, for other gas separation applications such as membrane gas absorption, the current CFD model should consider additional parameters such as the reaction rate of gas species along the membrane module. This is because membrane gas absorption involves both the gas permeation mechanism through membrane, as well as the chemical reaction of gas species in the absorption process.

4. Conclusion

A comparative study of film theory against the numerical approach by CFD was performed for predicting concentration polarisation and flux performance in membrane gas separation. This study shows that the film theory model becomes less accurate typically at high CP conditions when gas permeation increases across the membrane due to higher membrane selectivity and pressure ratio, leading to a large difference in CP predictions as well as flux performance. This suggests that the film theory is not recommended for membranes with high permeance or high-pressure conditions. Given that the typical range of feed composition and temperature has little impact on fluid properties, both film theory and CFD models predict CP and flux performance similarly. Overall, the analytical film theory can serve as a reliable approximation for membrane gas applications under low CP at high crossflow and low flux conditions. The results also indicate that film theory is most accurate in predicting CP in the region closer to the membrane entrance. Although this study is performed for the most widely studied CO_2/CH_4 gas separation, the same insights could be applied to other similar gas applications for process design improvement in dense membrane modules.

Declaration of Competing Interest

The authors declare that they have no known competing financial interests or personal relationships that could have appeared to influence the work reported in this paper.

Acknowledgements

The authors would like to acknowledge the funding support provided by Universiti Malaysia Pahang research grant (Reference code: PGRS1903134). One of us (K.F.) gratefully acknowledges the scholarship funding provided by Universiti Malaysia Pahang (UMP).

References

Ahmad, F., Lau, K.K., Lock, S.S.M., Rafiq, S., Khan, A.U., Lee, M., 2015. Hollow fiber membrane model for gas separation: process simulation, experimental validation and module characteristics study. J. Ind. Eng. Chem. 21, 1246–1257.

Alkhamis, N., Oztekin, D.E., Anqi, A.E., Alsaiari, A., Oztekin, A., 2015. Numerical study of gas separation using a membrane. Int. J. Heat. Mass Transf. 80, 835–843.

Al-Obaidi, M.A., Mujtaba, I.M., 2016. Steady state and dynamic modeling of spiral wound wastewater reverse osmosis process. Comput. Chem. Eng. 90, 278–299.

Baker, R.W., 2004. Membrane Technology and Applications. John Wiley & Sons Ltd, England.

Bhattacharya, S., Hwang, S.-T., 1997. Concentration polarization, separation factor, and Peclet number in membrane processes. J. Membr. Sci. 132, 73–90.

Bird, R.B., Stewart, W.E., Lightfoot, E.N., 1960. Transport Phenomena. John Wiley & Sons, New York.

Blinova, N.V., Svec, F., 2012. Functionalized polyaniline-based composite membranes with vastly improved performance for separation of carbon dioxide from methane. J. Membr. Sci. 423–424, 514–521.

Brian, P.L.T., 1965. Concentration polarization in reverse osmosis desalination with variable flux and incomplete salt rejection. Ind. Eng. Chem. Fundam. 4, 439–445.

Cakal, U., Yilmaz, L., Kalipcilar, H., 2012. Effect of feed gas composition on the separation of CO_2/CH_4 mixtures by PES-SAPO 34-HMA mixed matrix membranes. J. Membr. Sci. 417–418, 45–51.

Chen, W.-H., Syu, W.-Z., Hung, C.-I., 2011. Numerical characterization on concentration polarization of hydrogen permeation in a Pd-based membrane tube. Int. J. Hydrog. Energy 36, 14734–14744.

Chen, W.-H., Syu, W.-Z., Hung, C.-I., Lin, Y.-L., Yang, C.-C., 2012. A numerical approach of conjugate hydrogen permeation and polarization in a Pd membrane tube. Int. J. Hydrog. Energy 37, 12666–12679.

Cussler, E.L., 1997. Diffusion, Mass Transfer in Fluid Systems, 2nd Edition ed. The Press Syndicate of the University of Cambridge, United Kingdom.

Feng, F., Liang, C.-Z., Wu, J., Weber, M., Maletzko, C., Zhang, S., Chung, T.-S., 2021. Polyphenylsulfone (PPSU)-based copolymeric membranes: effects of chemical structure and content on gas permeation and separation. Polymers 13, 2745.

Fimbres-Weihs, G.A., Wiley, D.E., 2010. Review of 3D CFD modeling of flow and mass transfer in narrow spacer-filled channels in membrane modules. Chem. Eng. Process.: Process.Intensif. 49, 759–781.

Fletcher, D.F., Wiley, D.E., 2004. A computational fluids dynamics study of buoyancy effects in reverse osmosis. J. Membr. Sci. 245, 175–181.

He, G., Mi, Y., Lock Yue, P., Chen, G., 1999. Theoretical study on concentration polarization in gas separation membrane processes. J. Membr. Sci. 153, 243–258.

He, X., 2018. A review of material development in the field of carbon capture and the application of membrane-based processes in power plants and energy-intensive industries. Energy, Sustain. Soc. 8, 34.

Huang, Y., Merkel, T.C., Baker, R.W., 2014. Pressure ratio and its impact on membrane gas separation processes. J. Membr. Sci. 463, 33–40.

Liang, C.Z., Yong, W.F., Chung, T.-S., 2017. High-performance composite hollow fiber membrane for flue gas and air separations. J. Membr. Sci. 541, 367–377.

Liang, C.Z., Liu, J.T., Lai, J.-Y., Chung, T.-S., 2018. High-performance multiple-layer PIM composite hollow fiber membranes for gas separation. J. Membr. Sci. 563, 93–106.

Liang, Y.Y., Chapman, M.B., Fimbres-Weihs, G.A., Wiley, D.E., 2014. CFD modelling of electro-osmotic permeate flux enhancement on the feed side of a membrane module. J. Membr. Sci. 470, 378–388.

Liang, Y.Y., Fimbres-Weihs, G.A., Setiawan, R., Wiley, D.E., 2016. CFD modelling of unsteady electro-osmotic permeate flux enhancement in membrane systems. Chem. Eng. Sci. 146, 189–198.

Lüdtke, O., Behling, R.D., Ohlrogge, K., 1998. Concentration polarization in gas permeation. J. Membr. Sci. 146, 145–157.

Matthiasson, E., Sivik, B., 1980. Concentration polarization and fouling. Desalination 35, 59–103.
Michaels, A.S., 1968. New separation technique for the CPI. Chem. Engnineering Prog. 64, 31–42.
Moran, M.J., Shapiro, H.N., 1988. Fundamentals of engineering thermodynamics. John Wiley and Sons Inc, New York, NY, United States.
Mourgues, A., Sanchez, J., 2005. Theoretical analysis of concentration polarization in membrane modules for gas separation with feed inside the hollow-fibers. J. Membr. Sci. 252, 133–144.
Perry, R., Green, D., 2007. Perry's Chemical Engineers' Handbook, 8th illustrated ed. McGraw-Hill, New York.
Probstein, R.F., 1989. Physiochemical Hydrodynamics: An Introduction. John Wiley & Sons, Hoboken, New Jersey.
Probstein, R.F., Shen, J.S., Leung, W.F., 1977. Ultrafiltration of macromolecular solutions at high polarization in laminar channel flow. Desalination 24, 1–16.
Roache, P.J., Knupp, P.M., 1993. Completed Richardson extrapolation. Commun. Numer. Methods Eng. 9, 365–374.
Saedi, S., Madaeni, S.S., Hassanzadeh, K., Shamsabadi, A.A., Laki, S., 2014. The effect of polyurethane on the structure and performance of PES membrane for separation of carbon dioxide from methane. J. Ind. Eng. Chem. 20, 1916–1929.
Schwinge, J., Wiley, D.E., Fletcher, D.F., 2002a. Simulation of the flow around spacer filaments between channel walls. 2. Mass-transfer enhancement. Ind. Eng. Chem. Res. 41, 4879–4888.
Schwinge, J., Wiley, D.E., Fletcher, D.F., 2002b. Simulation of the flow around spacer filaments between narrow channel walls. 1. Hydrodynamics. Ind. Eng. Chem. Res. 41, 2977–2987.
Takaba, H., Nakao, S.-i, 2005. Computational fluid dynamics study on concentration polarization in H_2/CO separation membranes. J. Membr. Sci. 249, 83–88.
White, L.S., Blinka, T.A., Kloczewski, H.A., Wang, If, 1995. Properties of a polyimide gas separation membrane in natural gas streams. J. Membr. Sci. 103, 73–82.
Wiley, D.E., Fletcher, D.F., 2003. Techniques for computational fluid dynamics modelling of flow in membrane channels. J. Membr. Sci. 211, 127–137.
Wilke, C.R., 1950. A viscosity equation for gas mixtures. J. Chem. Phys. 18, 517–519.
Yu, L., Nobandegani, M.S., Hedlund, J., 2022. Industrially relevant CHA membranes for CO_2/CH_4 separation. J. Membr. Sci. 641, 119888.
Zhang, J., Liu, D., He, M., Xu, H., Li, W., 2006. Experimental and simulation studies on concentration polarization in H_2 enrichment by highly permeable and selective Pd membranes. J. Membr. Sci. 274, 83–91.
Zydney, A.L., 1997. Stagnant film model for concentration polarization in membrane systems. J. Membr. Sci. 130, 275–281.